

A family of Mn(II) complexes exhibiting strong photo- and triboluminescence as well as polymorphic luminescence

Alexander V. Artem'ev,^{*a} Maria P. Davydova,^a Mariana I. Rakhmanova,^a Irina Yu. Bagryanskaya,^b Denis P. Pishchur^a

^a Nikolaev Institute of Inorganic Chemistry, SB RAS, 3, Acad. Lavrentiev Ave., 630090 Novosibirsk, Russian Federation

^b N. N. Vorozhtsov Novosibirsk Institute of Organic Chemistry, SB RAS, 9, Acad. Lavrentiev Ave., Novosibirsk 630090, Russian Federation

*E-mail: chemisufarm@yandex.ru (Alexander V. Artem'ev)

Table of content

S2–3	§1. Experimental details
S4–10	§2. Single crystal X-ray crystallography
S11–13	§3. Powder X-ray diffraction patterns
S14	§4. FT-IR spectra
S15	§5. Thermogravimetric analysis
S16–18	§6. DSC analysis
S19–23	§7. Temperature-dependant excitation and emission spectra
S24	§8. Attempts to interconvert 2g and 2y
S25	§9. References

§1. Experimental details

All reactions were carried out under ambient conditions (23–25 °C, air). Pro-ligands **L¹** and **L²** were synthesized by oxidation of the Xantphos (99%, Dalchem) and *t*-Bu-Xantphos (99%, Dalchem), respectively, in H₂O₂/H₂O/acetone system. MnCl₂·4H₂O, MnBr₂·4H₂O (98%, Aldrich) and MnI₂ (99.9%, Aldrich) were used as purchased.

The microanalyses were performed on a MICRO cube analyzer.

Powder X-ray diffraction analyses (PXRD) were performed on a Shimadzu XRD-7000 diffractometer (Cu-K α radiation, Ni – filter, 3–35° 2 θ range, 0.03° 2 θ step, 5 s per point).

Thermogravimetric analyses (TGA&DTG&c-DTA) were carried out in a closed Al₂O₃ pan under argon flow at 10 °C/min⁻¹ heating rate using a NETZSCH STA 449 F1 Jupiter STA up to 600 °C.

DSC measurements were carried out on NETZSCH 204 F1 Phoenix using heat flow measurement method at a 9 K min⁻¹ heating rate in 25 ml min⁻¹ Ar flux in a sealed aluminum crucible with lid. Netzsch Proteus Analysis software was used to determine the DSC peak area and transition temperatures. Recent recommendations on DSC calibrations were taken into account.^[1]

FT-IR spectra were recorded on a Bruker Vertex 80 spectrometer at ambient temperature.

Excitation and emission spectra were recorded on a Fluorolog 3 spectrometer (Horiba Jobin Yvon) equipped with a cooled PC177CE-010 photon detection module and an R2658 photomultiplier. The emission decays were recorded on the same instrument. The absolute PLQYs were determined at 300 K using a Fluorolog 3 Quanta-phi integrating sphere. Temperature-dependant excitation and emission spectra as well as emission decays were recorded using an Optistat DN optical cryostat (Oxford Instruments) integrated with above spectrometer.

Synthesis and characterization data for compounds 1–6

[Mn(L¹)Cl₂] (1). To a solution of pro-ligand **L¹** (60 mg, 0.098 mmol) in CH₂Cl₂ (1 mL), a solution of MnCl₂·4H₂O (19 mg, 0.098 mmol) in EtOH (1 mL) was added and the mixture was stirred for 1 h. Diethyl ether (10 mL) was then added to a resulting solution before the precipitate formed was centrifuged and dried on air. White powder. Yield: 65 mg (90%). FT-IR (KBr, cm⁻¹): 399 (w), 430 (m), 455 (w), 478 (w), 500 (m), 527 (s), 540 (s), 546 (s), 557 (s), 588 (m), 604 (w), 619 (w), 691 (s), 698 (s), 714 (m), 723 (s), 746 (s), 766 (m), 789 (s), 880 (m), 999 (m), 1028 (w), 1070 (m), 1084 (m), 1099 (m), 1121 (s), 1130 (s), 1144 (s), 1161 (s), 1175 (s), 1202 (w), 1240 (vs), 1288 (w), 1333 (w), 1368 (w), 1410 (vs), 1439 (s), 1476 (w), 1485 (w), 1574 (m), 1589 (m), 1611 (m), 2868 (w), 2928 (w), 2965 (m), 3026 (w), 3038 (w), 3053 (w), 3075 (w). Anal. Calc. for C₃₉H₃₂Cl₂MnO₃P₂ (736.46): C, 63.6; H, 4.4. Found: C, 63.4; H, 4.4.

[Mn(L¹)Br₂] (2g). The procedure was similar to that for **1** except that MnBr₂·4H₂O (42 mg, 0.147 mmol) and **L¹** (60 mg, 0.098 mmol) were used. Greenish powder. Yield: 67 mg (83%). FT-IR (KBr, cm⁻¹): 399 (w), 424 (w), 455 (w), 494 (m), 528 (s), 542 (vs), 561 (s), 577 (w), 586 (w), 604 (vw), 691 (s), 712 (m), 723 (s), 748 (s), 787 (s), 802 (m), 876 (m), 955 (w), 997 (m), 1028 (w), 1069 (w), 1084 (w), 1101 (m), 1119 (s), 1128 (s), 1144 (m), 1161 (s), 1177 (s), 1227 (vs), 1246 (m), 1283 (w), 1364 (w), 1402 (vs), 1437 (s), 1462 (w), 1476 (w), 1483 (w), 1574 (w), 1589 (m), 1611 (m), 2957 (w), 2974 (w), 3053 (w). Anal. Calc. for C₃₉H₃₂Br₂MnO₃P₂ (825.36): C, 56.7; H, 3.9. Found: C, 56.9; H, 3.9.

[Mn(L¹)Br₂] (2y). The procedure was similar to that for **1** except that MnBr₂·4H₂O (28 mg, 0.098 mmol) and **L¹** (60 mg, 0.098 mmol) were used. Yellowish powder. Yield: 60 mg (74%). FT-IR (KBr, cm⁻¹): 399 (w), 424 (w),

455 (w), 494 (m), 528 (s), 542 (vs), 561 (s), 577 (w), 586 (w), 604 (vw), 691 (s), 712 (m), 723 (s), 748 (s), 787 (s), 802 (m), 876 (m), 955 (w), 997 (m), 1028 (w), 1069 (w), 1084 (w), 1101 (m), 1119 (s), 1128 (s), 1144 (m), 1161 (s), 1177 (s), 1227 (vs), 1246 (m), 1283 (w), 1364 (w), 1402 (vs), 1437 (s), 1462 (w), 1476 (w), 1483 (w), 1574 (w), 1589 (m), 1611 (m), 2957 (w), 2974 (w), 3053 (w). Anal. Calc. for $C_{39}H_{32}Br_2MnO_3P_2$ (825.36): C, 56.7; H, 3.9. Found: C, 56.8; H, 3.9.

[Mn(L¹)I₂] (3). The procedure was similar to that for **1** except that MnI₂ (30 mg, 0.098 mmol) and L¹ (60 mg, 0.098 mmol) were used. Yellow powder. Yield: 70 mg (78%). FT-IR (KBr, cm⁻¹): 399 (w), 424 (w), 455 (w), 494 (m), 530 (s), 540 (vs), 561 (s), 586 (w), 606 (vw), 617 (vw), 689 (s), 712 (m), 723 (s), 748 (s), 789 (s), 799 (m), 818 (vw), 847 (vw), 874 (w), 997 (m), 1028 (w), 1069 (w), 1086 (vw), 1103 (m), 1121 (s), 1128 (s), 1144 (m), 1161 (s), 1177 (s), 1225 (s), 1246 (m), 1285 (vw), 1314 (w), 1333 (w), 1362 (w), 1402 (vs), 1437 (s), 1472 (w), 1483 (w), 1572 (w), 1589 (m), 1607 (m), 2858 (vw), 2924 (w), 2957 (w), 2978 (w), 2990 (vw), 3053 (w), 3078 (vw), 3402 (m). Anal. Calc. for $C_{39}H_{32}I_2MnO_3P_2$ (919.36): C, 50.9; H, 3.5. Found: C, 50.9; H, 3.3.

[Mn(L²)Br₂] (4). To a solution of pro-ligand L² (60 mg, 0.113 mmol) in CH₂Cl₂ (1 mL), a solution of MnBr₂·4H₂O (32 mg, 0.113 mmol) in EtOH (1 mL) was added. The reaction mixture was stirred for 1 h, then diethyl ether (10 mL) was added to the resulting solution. The precipitate formed, according to PXRD data, represented a mixture of **4** and **5**·CH₂Cl₂·H₂O. This mixture was re-dissolved in CH₂Cl₂, and the solution was kept in diethyl ether at ambient temperature for overnight to give a mixture of single crystals of **4** and **5**·CH₂Cl₂·H₂O. Using a microscope and a UV-lamp, the mixture was mechanically separated into the individual phases. Yield of **4**: 36 mg (43%). Yield of **5**·CH₂Cl₂·H₂O: 35 mg (40%). Yellowish crystals. FT-IR (KBr, cm⁻¹): 469 (w), 494 (m), 513 (m), 530 (m), 542 (w), 592 (m), 687 (w), 754 (m), 785 (m), 799 (m), 808 (m), 818 (m), 864 (w), 1084 (w), 1126 (m), 1155 (m), 1190 (m), 1207 (s), 1242 (m), 1371 (m), 1393 (vs), 1477 (m), 1597 (w), 2872 (m), 2905 (m), 2930 (m), 2953 (m), 2963 (m), 2972 (m), 2997 (m), 3410 (w). Anal. Calc. for $C_{31}H_{49}Br_2MnO_3P_2$ (746.40): C, 49.9; H, 6.6. Found: C, 50.0; H, 6.5.

(L²·H)₂MnBr₄·CH₂Cl₂·H₂O (5)·CH₂Cl₂·H₂O. To a solution of pro-ligand L² (60 mg, 0.113 mmol) in CH₂Cl₂ (1 mL), a solution of MnBr₂·4H₂O (16 mg, 0.056 mmol) in EtOH (1 mL) was added along with some drops of aqueous HBr (48%). The mixture was stirred for 1 h, and diethyl ether (10 mL) then was added to the resulting solution. The precipitate formed was centrifuged and dried on air. Yellowish powder. Yield: 67 mg (77%). FT-IR (KBr, cm⁻¹): 438 (w), 457 (w), 478 (w), 494 (w), 527 (w), 565 (w), 594 (w), 658 (m), 748 (m), 783 (m), 804 (m), 880 (m), 905 (s), 953 (m), 1022 (w), 1084 (w), 1124 (w), 1152 (w), 1186 (w), 1244 (m), 1279 (w), 1306 (w), 1375 (m), 1408 (vs), 1477 (m), 1607 (w), 1636 (w), 2870 (w), 2934 (w), 2970 (m), 3485 (w). Anal. Calc. for $C_{63}H_{102}Br_4Cl_2MnO_7P_4$ (1540.83): C, 49.1; H, 6.7. Found: C, 49.3; H, 6.5.

(L²·H)₂MnI₄ (6). The procedure was similar to that for **4** except that MnI₂ (17 mg, 0.056 mmol) and L² (60 mg, 0.113 mmol) were used. Yellowish powder. Yield: 80 mg (87%). FT-IR (KBr, cm⁻¹): 420 (w), 438 (m), 457 (w), 478 (m), 494 (w), 513 (w), 527 (w), 538 (w), 563 (w), 594 (m), 658 (m), 750 (m), 785 (m), 804 (m), 878 (s), 899 (s), 930 (m), 951 (m), 1020 (w), 1084 (w), 1123 (w), 1150 (w), 1188 (w), 1244 (s), 1275 (w), 1304 (w), 1375 (m), 1400 (vs), 1477 (m), 1605 (m), 1624 (w), 2870 (w), 2907 (vw), 2926 (vw), 2968 (m), 2976 (m), 2997 (w), 3393 (s). Anal. Calc. for $C_{62}H_{98}I_4MnO_6P_4$ (1625.89): C, 45.8; H, 6.1. Found: C, 45.9; H, 6.3.

§2. Single crystal X-ray crystallography

The single crystals of the above complexes were grown by vapor diffusion of diethyl ether into the CH₂Cl₂ solutions at ambient temperature for overnight. The data were collected on a Bruker Kappa Apex II CCD diffractometer using ϕ, ω -scans of narrow (0.5°) frames with MoK α radiation ($\lambda = 0.71073 \text{ \AA}$) and a graphite monochromator. The structures were solved by direct methods SHELXL97 and refined by a full matrix least-squares anisotropic-isotropic (for H atoms) procedure using SHELXL-2014/7 programs set.^[2] Absorption corrections were applied using the empirical multiscan method with the SADABS program.^[3] The positions of the hydrogen atoms were calculated with the riding model.

The crystallographic data and details of the refinements for **1–6** are summarized in **Table S1**. CCDC 1984715–1984718 and 1984720–1984722 contain the supplementary crystallographic data for this paper. These data can be obtained free of charge from The Cambridge Crystallographic Data Center at http://www.ccdc.cam.ac.uk/data_request/cif

Table S1. X-Ray crystallographic data for **1–6**.

Compound	1	2g	2y	3	4	5·CH₂Cl₂·H₂O	6
CCDC number	1984715	1984716	1984717	1984718	1984720	1984721	1984722
Chemical formula	C ₃₉ H ₃₂ Cl ₂ MnO ₃ P ₂	C ₃₉ H ₃₂ Br ₂ MnO ₃ P ₂	C ₃₉ H ₃₂ Br ₂ MnO ₃ P ₂	C ₃₉ H ₃₂ I ₂ MnO ₃ P ₂	C ₃₁ H ₄₉ Br ₂ MnO ₃ P ₂	C ₆₃ H ₁₀₂ Br ₄ Cl ₂ MnO ₇ P ₄	C ₆₂ H ₉₈ I ₄ MnO ₆ P ₄
<i>M</i> _r	736.42	825.34	825.34	919.32	746.40	1540.80	1625.82
Crystal system, space group	Monoclinic, <i>P</i> 2 ₁ / <i>n</i>	Triclinic, <i>P</i> ̄1	Monoclinic, <i>P</i> 2 ₁ / <i>n</i>	Monoclinic, <i>P</i> 2 ₁ / <i>c</i>	Monoclinic, <i>P</i> 2 ₁ / <i>n</i>	Triclinic, <i>P</i> ̄1	Triclinic, <i>P</i> ̄1
Temperature (K)	296	296	200	200	298	296	296
<i>a</i> , <i>b</i> , <i>c</i> (Å)	14.3629(10), 17.0889(13), 15.1872(10)	10.7909(3), 11.3448(2), 17.5671(4)	14.5868(6), 17.0770(8), 15.1797(7)	18.7759(8), 11.7061(5), 19.4706(7)	11.9082(6), 17.4243(7), 17.2561(10)	12.7707(16), 12.8650(15), 25.667(3)	12.1784(6), 14.0345(5), 22.2697(10)
α, β, γ (°)	106.540(2)	95.226(1), 103.329(1), 116.304(1)	106.238(2)	117.670(1)	104.635(2)	90.462(7), 92.520(7), 119.608(6)	74.761(2), 79.927(2), 75.404(2)
<i>V</i> (Å ³)	3573.4(4)	1829.35(7)	3630.4(3)	3790.1(3)	3464.3(3)	3660.7(8)	3529.8(3)
<i>Z</i>	4	2	4	4	4	2	2
μ (mm ⁻¹)	0.65	2.67	2.69	2.10	2.81	2.57	2.07
Crystal size (mm)	0.90 × 0.20 × 0.10	0.20 × 0.20 × 0.15	0.90 × 0.15 × 0.10	0.40 × 0.40 × 0.30	0.60 × 0.40 × 0.15	0.90 × 0.60 × 0.02	0.50 × 0.30 × 0.02
<i>T</i> _{min} , <i>T</i> _{max}	0.768, 0.862	0.827, 0.928	0.455, 0.862	0.761, 0.862	0.614, 0.928	0.801, 0.928	0.801, 0.928
No. of measured, independent and observed [<i>I</i> > 2σ (<i>I</i>)] reflections	66146, 9971, 6603	28694, 9505, 7183	69412, 10113, 7617	67590, 10527, 8926	30660, 8942, 6334	61785, 16913, 9902	55601, 18334, 10240
<i>R</i> _{int}	0.060	0.037	0.055	0.042	0.063	0.066	0.041
(sin θ/λ) _{max} (Å ⁻¹)	0.705	0.705	0.705	0.705	0.705	0.654	0.706
<i>R</i> [<i>F</i> ² > 2σ(<i>F</i> ²)], <i>wR</i> (<i>F</i> ²), <i>S</i>	0.040, 0.112, 1.04	0.040, 0.111, 1.02	0.031, 0.084, 0.99	0.031, 0.083, 1.05	0.055, 0.154, 1.01	0.064, 0.185, 1.01	0.050, 0.118, 1.01
No. of reflections	9971	9505	10113	10527	8942	16913	18334
No. of parameters	426	424	426	426	366	768	728
No. of restraints	0	0	0	0	0	3	0
Δ <i>ρ</i> _{max} , Δ <i>ρ</i> _{min} (ε Å ⁻³)	0.32, -0.33	0.97, -1.12	0.52, -0.75	1.43, -1.80	0.97, -0.89	0.92, -0.93	1.35, -1.21

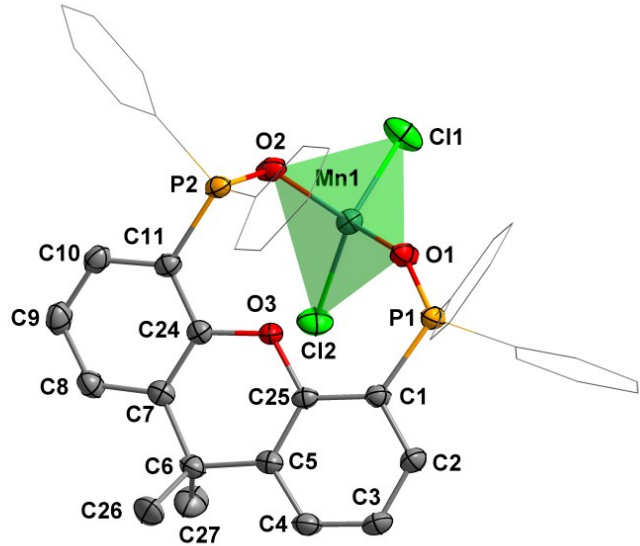


Figure S1. Molecular structure of **1**. Hydrogen atoms are omitted for clarity. Selected distances [Å] and angles (°): Mn1–O2 2.0511(15), Mn1–O1 2.0518(14), Mn1–Cl2 2.3244(7), Mn1–Cl1 2.3314(7), P1–O1 1.4968(15), P2–O2 1.5020(16); O2–Mn1–O1 96.20(7), O2–Mn1–Cl2 116.32(5), O1–Mn1–Cl2 107.68(5), O2–Mn1–Cl1 104.60(5), O1–Mn1–Cl1 116.59(5), Cl2–Mn1–Cl1 114.37(3).

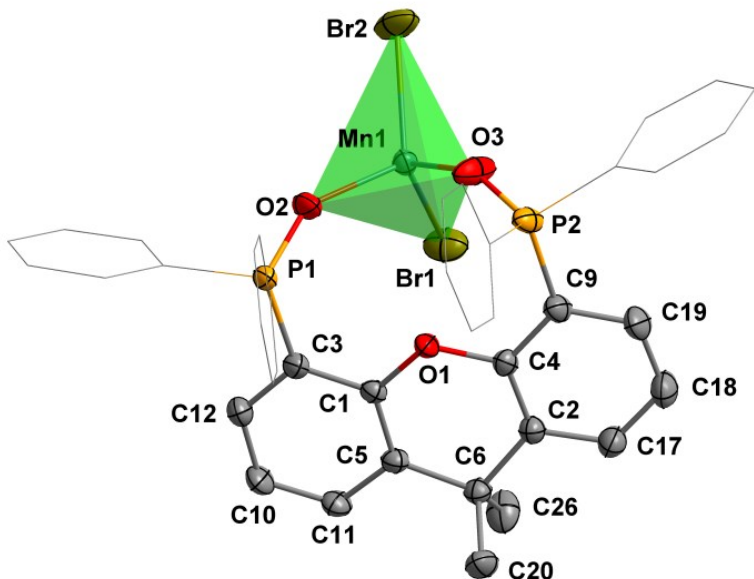


Figure S2. Molecular structure of **2g**. Hydrogen atoms are omitted for clarity. Selected distances [Å] and angles (°): Br1–Mn1 2.4671(5), Br2–Mn1 2.4535(5), Mn1–O3 2.021(2), Mn1–O2 2.0334(17), P1–O2 1.4978(18), P2–O3 1.488(2); O3–Mn1–O2 96.57(11), O3–Mn1–Br2 107.97(6), O2–Mn1–Br2 114.52(6), O3–Mn1–Br1 114.15(7), O2–Mn1–Br1 110.75(6), Br2–Mn1–Br1 112.024(18).

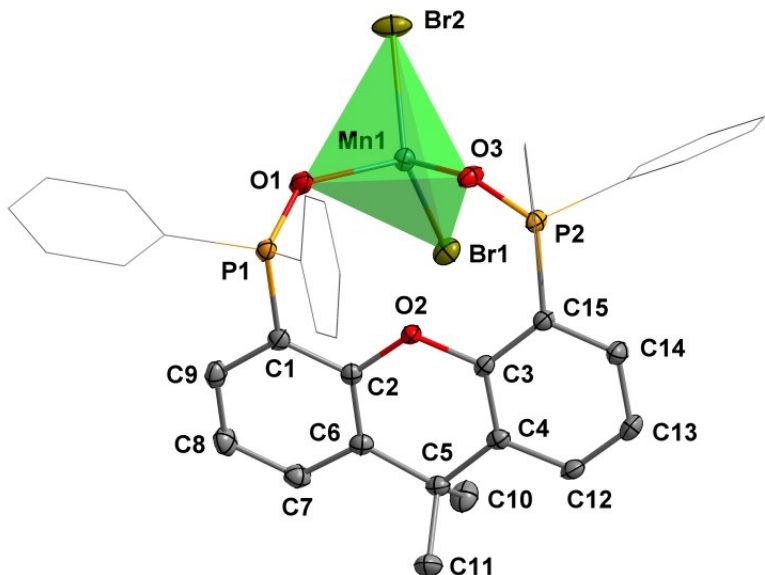


Figure S3. Molecular structure of **2y**. Hydrogen atoms are omitted for clarity. Selected distances [Å] and angles (°): Br1–Mn1 2.4699(4), Br2–Mn1 2.4744(4), Mn1–O3 2.0406(14), Mn1–O1 2.0431(14), P1–O1 1.5049(15), P2–O3 1.5041(14); O3–Mn1–O1 96.44(6), O3–Mn1–Br1 108.16(4), O1–Mn1–Br1 115.58(5), O3–Mn1–Br2 117.83(4), O1–Mn1–Br2 105.09(4), Br1–Mn1–Br2 112.908(13).

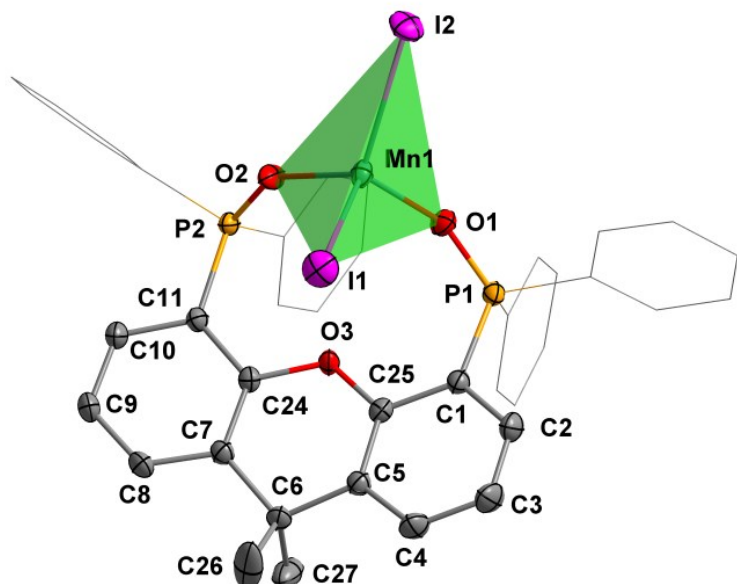


Figure S4. Molecular structure of **3**. Hydrogen atoms are omitted for clarity. Selected distances [Å] and angles (°): I1–Mn1 2.6685(4), I2–Mn1 2.6686(4), Mn1–O2 2.0124(15), Mn1–O1 2.0216(15), P1–O1 1.4990(15), P2–O2 1.5000(15); O2–Mn1–O1 97.23(7), O2–Mn1–I1 105.38(5), O1–Mn1–I1 112.61(5), O2–Mn1–I2 111.16(5), O1–Mn1–I2 107.62(5), I1–Mn1–I2 120.379(13).

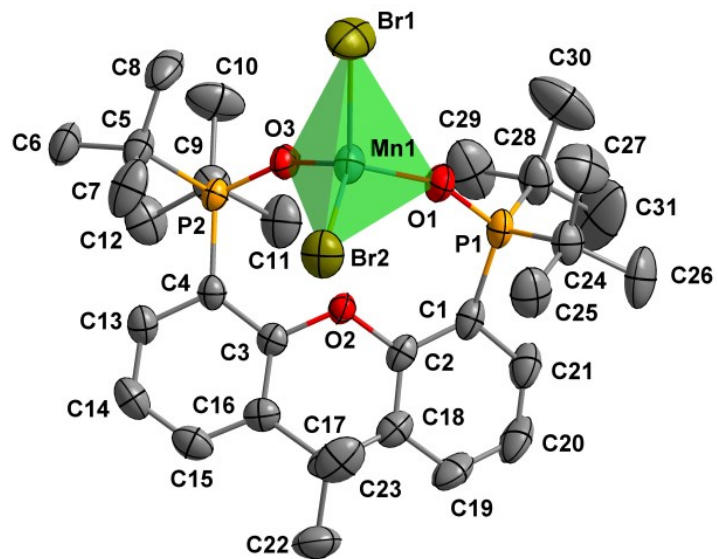


Figure S5. Molecular structure of **4**. Hydrogen atoms are omitted for clarity. Selected distances [Å] and angles (°): Br1–Mn1 2.4831(7), Br2–Mn1 2.4942(7), Mn1–O1 2.009(2), Mn1–O3 2.024(2), P1–O1 1.496(2), P2–O3 1.502(2); O1–Mn1–O3 92.11(10), O1–Mn1–Br1 111.25(8), O3–Mn1–Br1 107.72(7), O1–Mn1–Br2 116.32(8), O3–Mn1–Br2 119.38(7), Br1–Mn1–Br2 108.99(3).

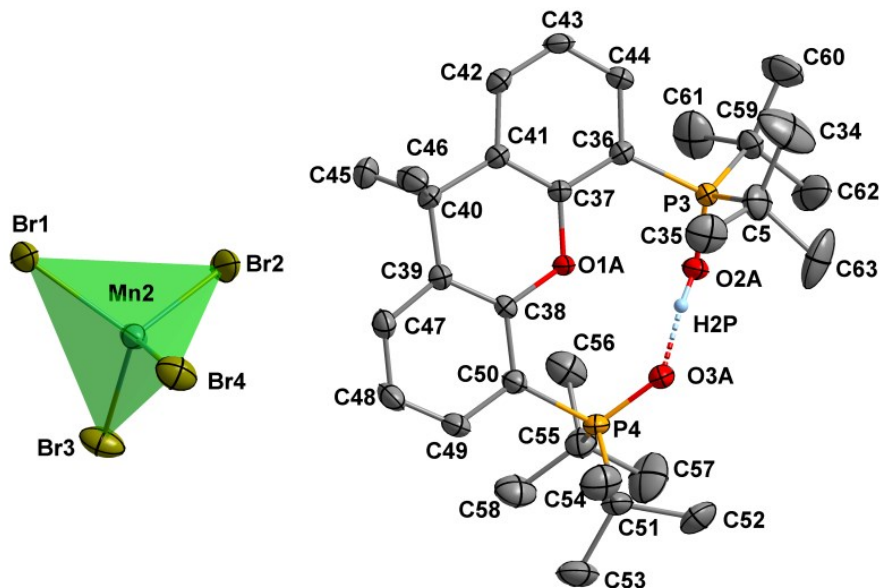


Figure S6. Molecular structure of **5·CH₂Cl₂·H₂O**. Hydrogen atoms and solvate molecules are omitted for clarity. Selected distances [Å] and angles (°): Br1–Mn2 2.5290(10), Br2–Mn2 2.4903(10), Br3–Mn2 2.5231(10), Br4–Mn2 2.4923(11), P1–O3 1.517(3), P2–O2 1.514(4), O2–H1P 0.74(6); Br2–Mn2–Br4 112.87(4), Br2–Mn2–Br3 105.89(4), Br4–Mn2–Br3 112.63(4), Br2–Mn2–Br1 107.17(4), Br4–Mn2–Br1 108.66(4), Br3–Mn2–Br1 109.42(4).

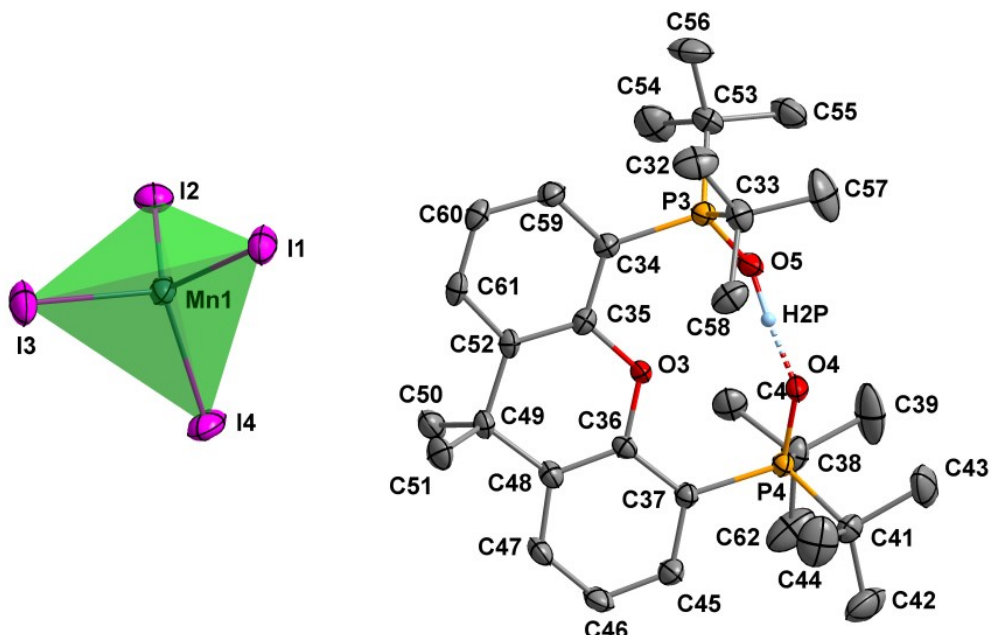


Figure S7. Molecular structure of **6**. Hydrogen atoms are omitted for clarity. Selected distances [Å] and angles (°): I1–Mn1 2.7300(8), I2–Mn1 2.7401(9), I3–Mn1 2.7134(8), I4–Mn1 2.6902(8), P1–O1 1.522(3), P2–O2 1.502(3), P3–O5 1.513(3), P4–O4 1.525(3), O2–H1P 0.97(5); I4–Mn1–I3 109.53(3), I4–Mn1–I1 109.15(3), I3–Mn1–I1 109.87(3), I4–Mn1–I2 105.03(3), I3–Mn1–I2 108.13(3), I1–Mn1–I2 114.96(3).

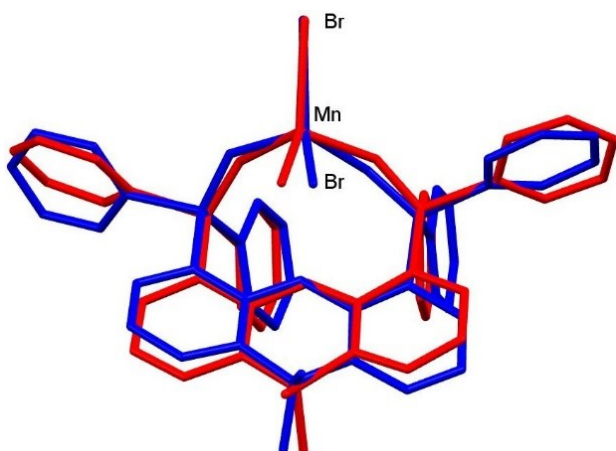
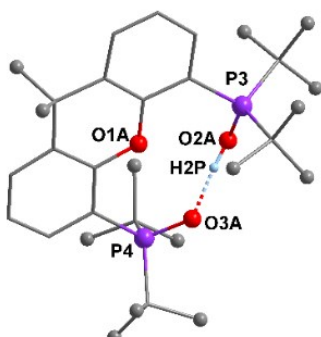


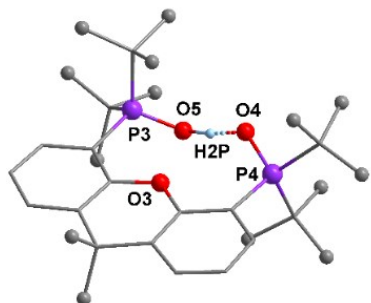
Figure S8. Overlayed structures of the complex $[\text{Mn}(\text{L}^1)\text{Br}_2]$ in polymorphs **2g** (red-colored) and **2y** (blue-colored).

Table S2. Parameters of hydrogen bond in the $[\text{L}^2\cdot\text{H}]^+$ cation of **5**· $\text{CH}_2\text{Cl}_2\cdot\text{H}_2\text{O}$.



D–H···A	D–H	H···A	D···A	D–H···A
O2A–H2P···O3A	0.8547(6)	1.5434(6)	2.3955(5)	174.459(6)

Table S3. Parameters of hydrogen bond in the $[L^2 \cdot H]^+$ cation of **6**.



D—H···A	D—H	H···A	D···A	D—H···A
O5—H2P···O4	1.0397(5)	1.3638(6)	2.3998(4)	173.567(5)

§3. Powder X-ray diffraction patterns

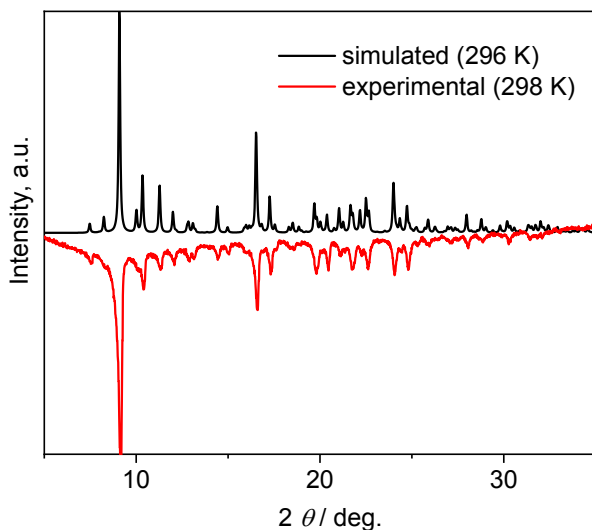


Figure S9. Experimental and simulated PXRD patterns of **1**.

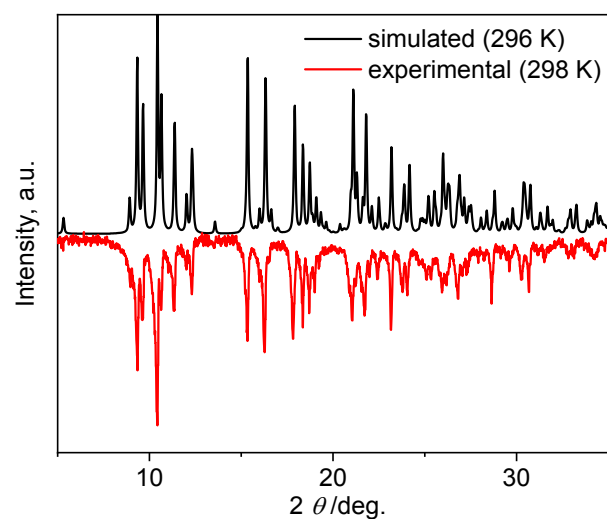


Figure S10. Experimental and simulated PXRD patterns of **2g**.

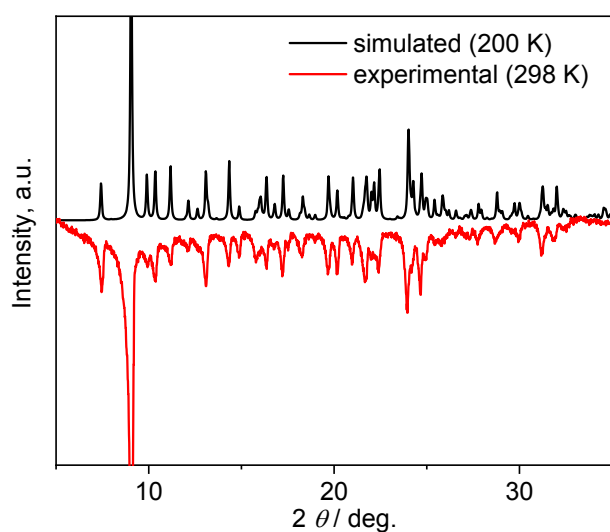


Figure S11. Experimental and simulated PXRD patterns of **2y**.

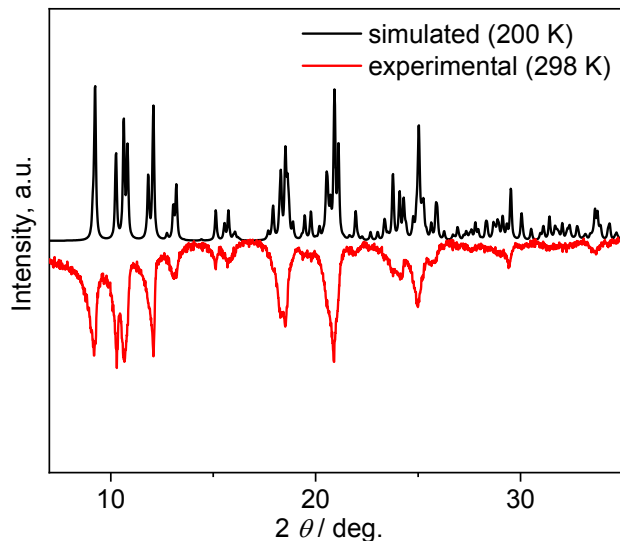


Figure S12. Experimental and simulated PXRD patterns of **3**.

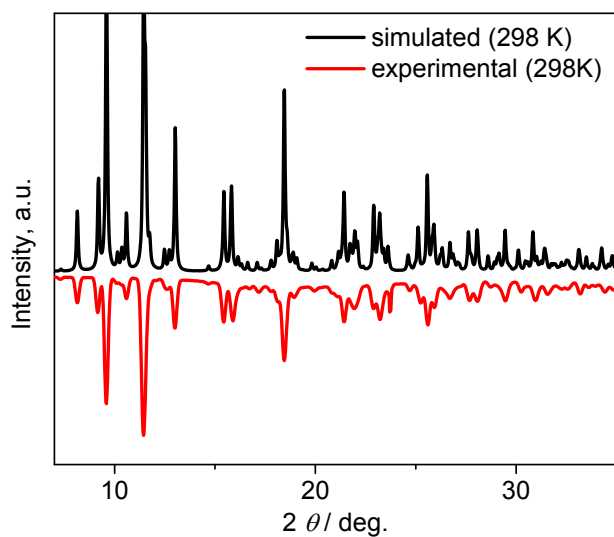


Figure S13. Experimental and simulated PXRD patterns of **4**.

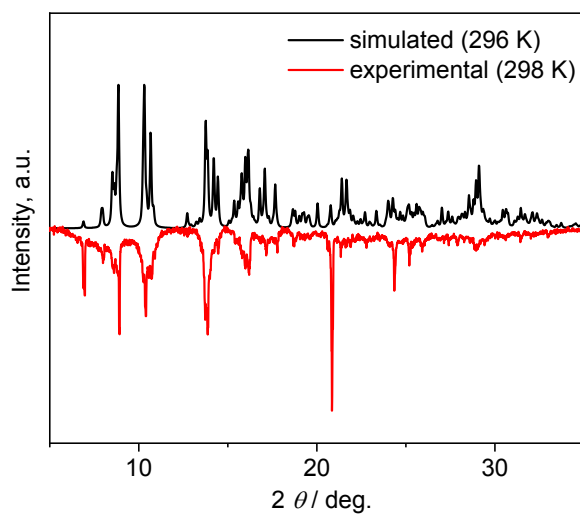


Figure S14. Experimental and simulated PXRD patterns of **5·CH₂Cl₂·H₂O**.

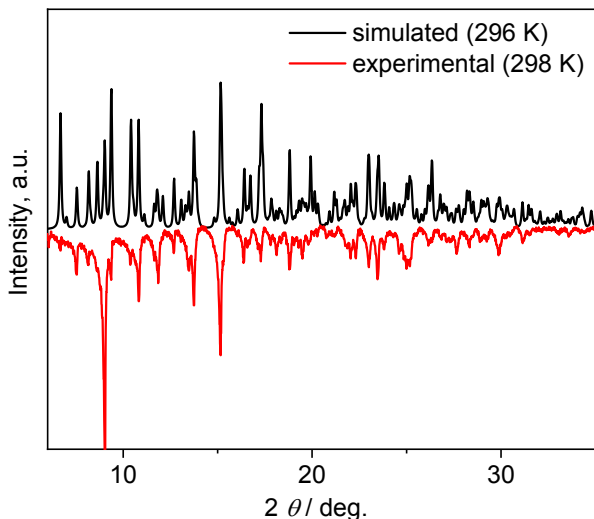


Figure S15. Experimental and simulated PXRD patterns of **6**.

§4. FT-IR spectra

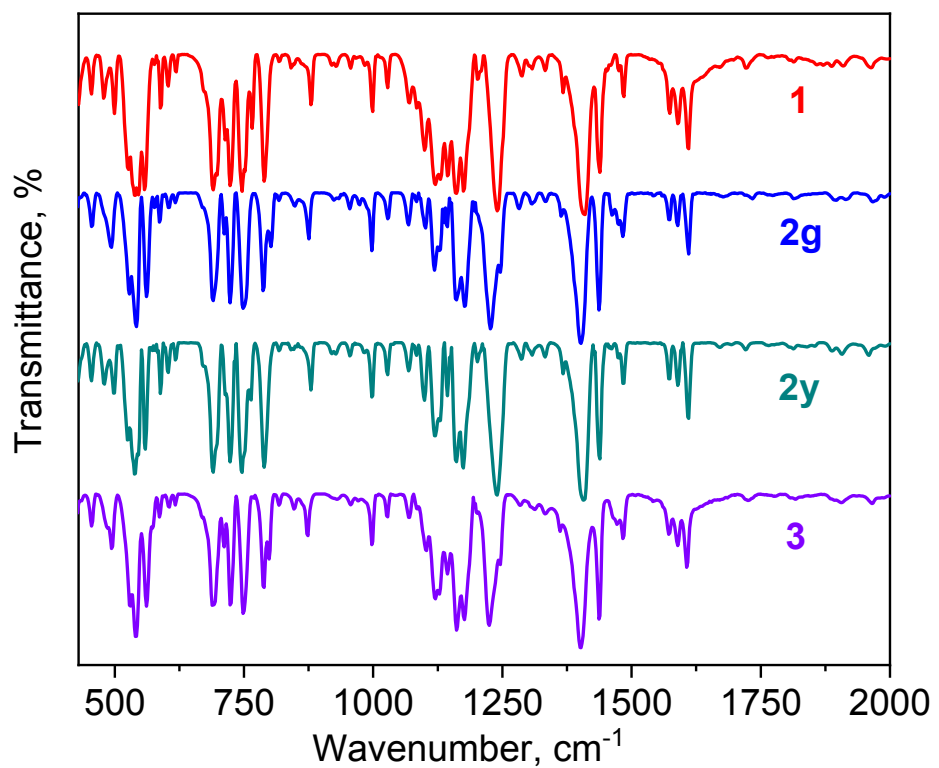


Figure S16. FT-IR spectra of **1–3** showed in the fingerprint region.

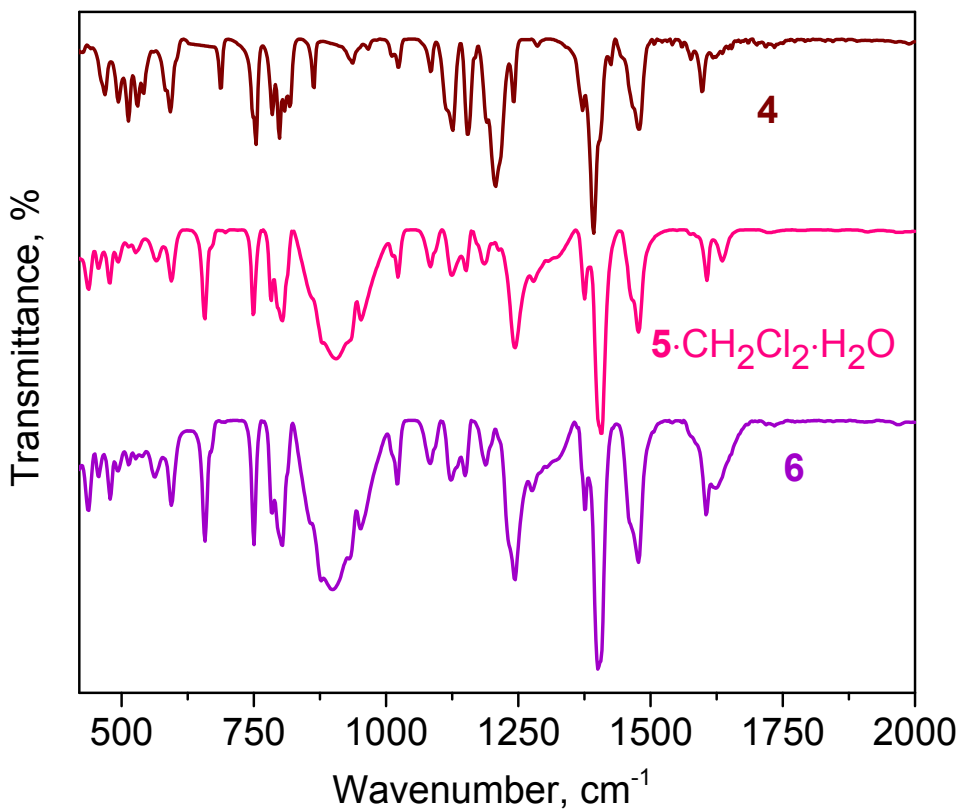


Figure S17. FT-IR spectra of **4–6** showed in the fingerprint region.

§5. Thermogravimetric analysis

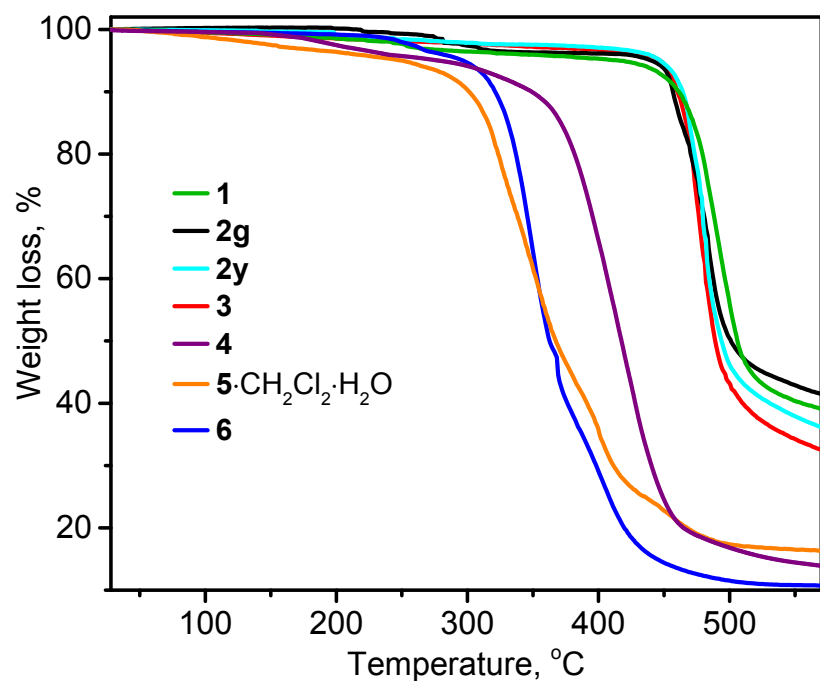


Figure S18. TGA curves for complexes **1–6**.

§6. DSC analysis

Table S4. Thermodynamic properties of complexes **1–6**.

Complex	Temperature range	Thermal anomalies		Type of anomaly	Irreversibility
		T _{onset} (K)	ΔH (J/g ⁻¹)		
1	300–520 K	—	—	—	—
2g		—	—	—	—
2y		378.1	0.7 ±0.1	1-st order	+
3		—	—	—	—
4		441.9±0.1	2.1±0.1	1-st order	+
5·H₂O·CH₂Cl₂		441.7±0.1	24.0±0.1	1-st order	+
6		513.4±0.1	19.6±0.8	decomposition	+

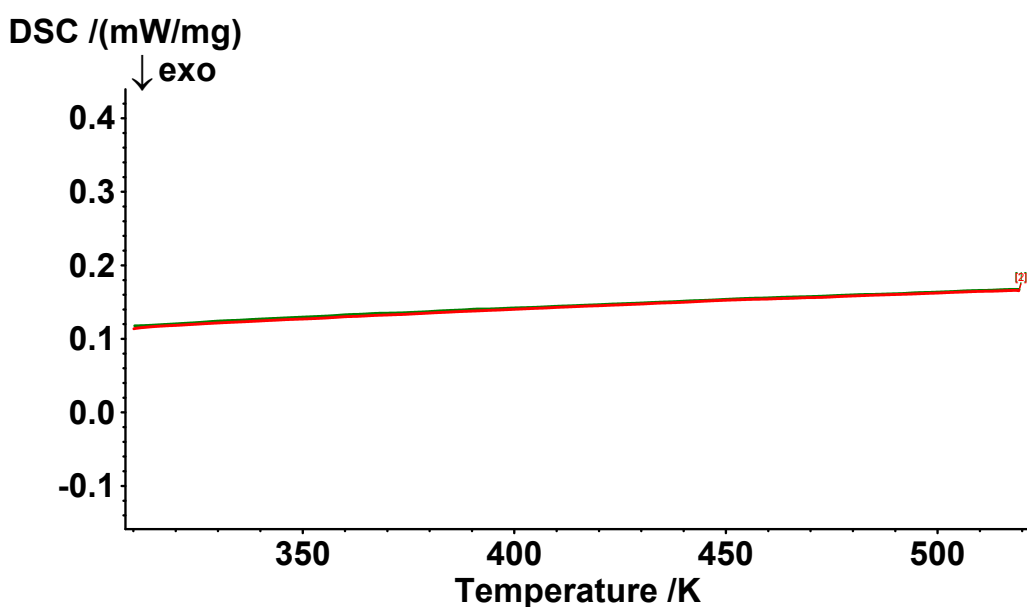


Figure S19. DSC curve for solid **1**.

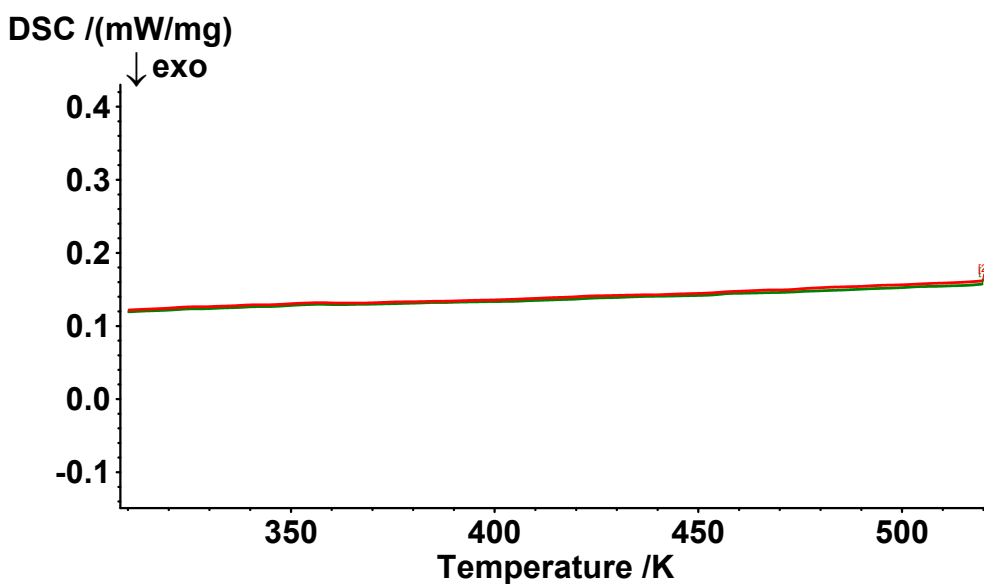


Figure S20. DSC curve for solid **2g**.

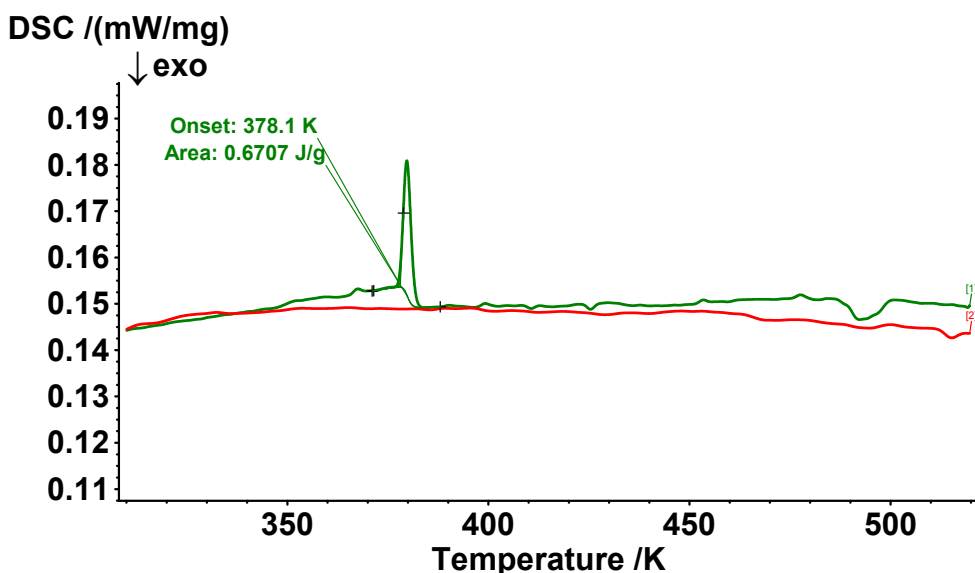


Figure S21. DSC curve for solid 2y.

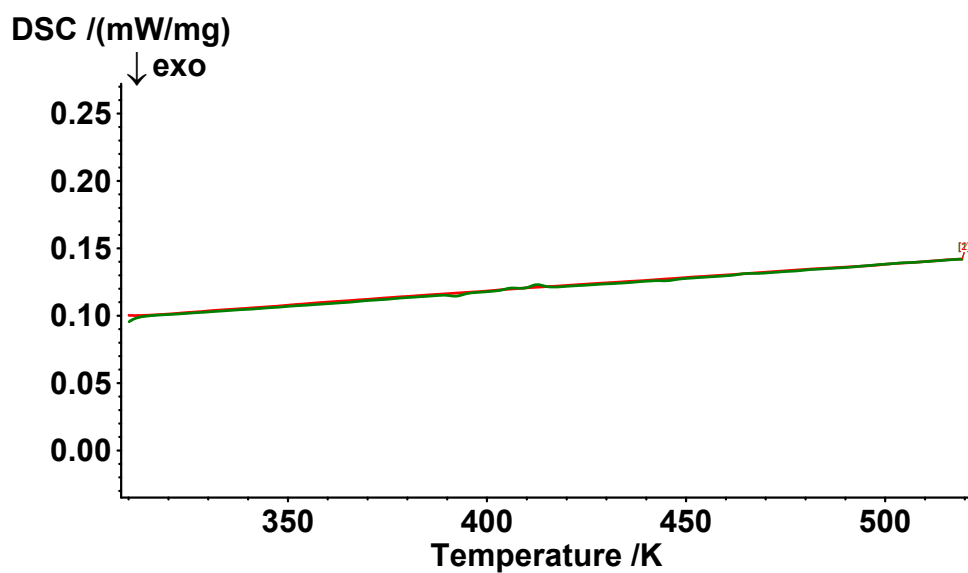


Figure S22. DSC curve for solid 3.

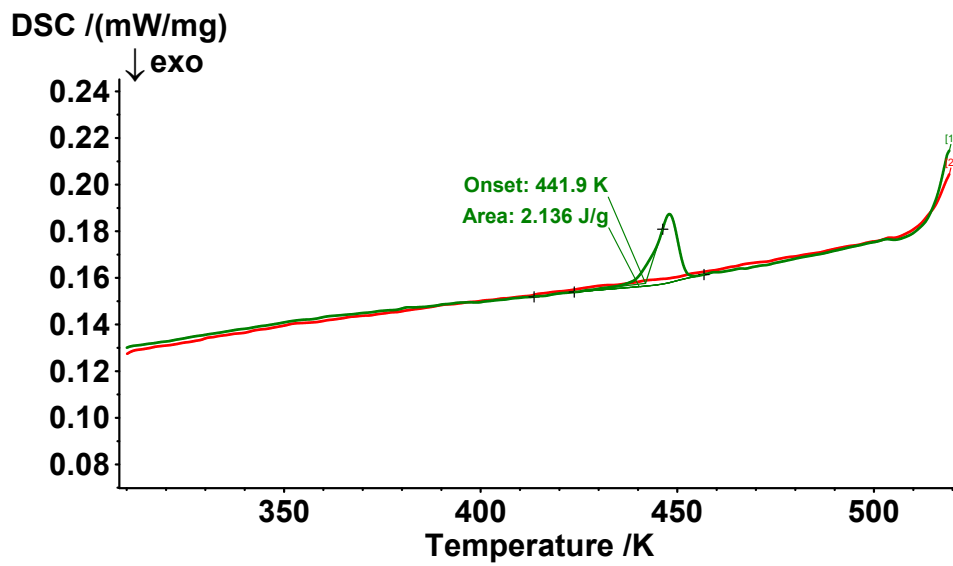


Figure S23. DSC curve for solid 4.

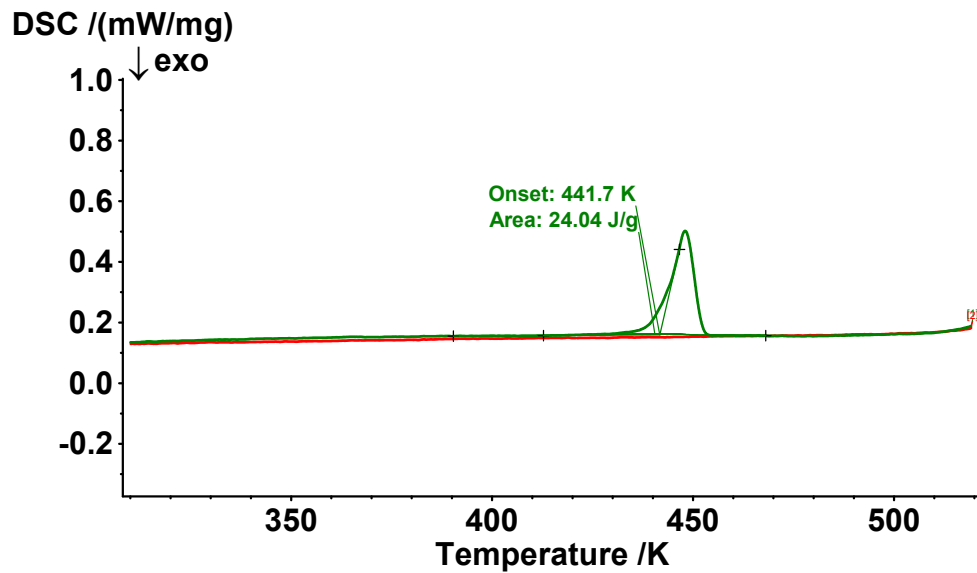


Figure S24. DSC curve for solid $5 \cdot \text{CH}_2\text{Cl}_2 \cdot \text{H}_2\text{O}$.

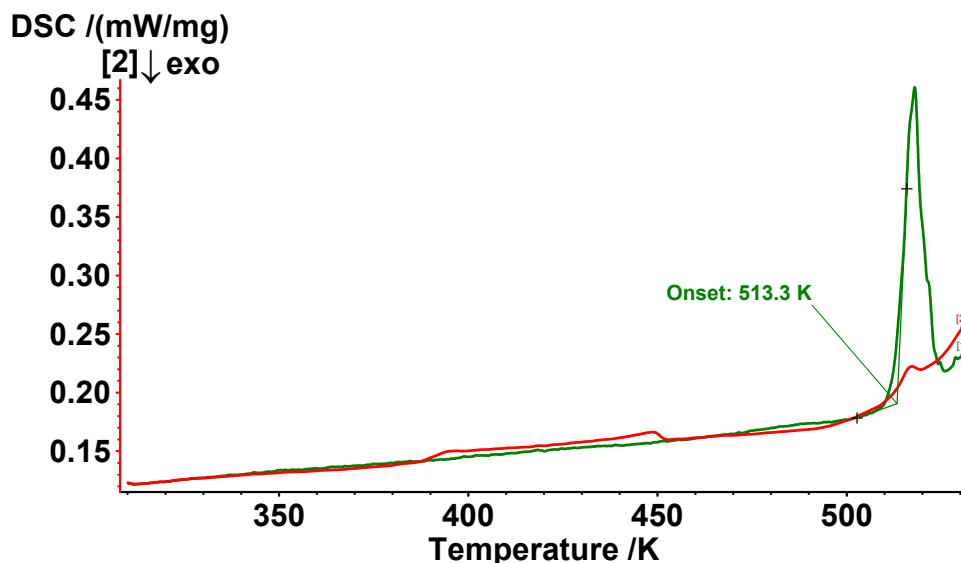


Figure S25. DSC curve for solid 6.

§7. Temperature-dependant excitation and emission spectra

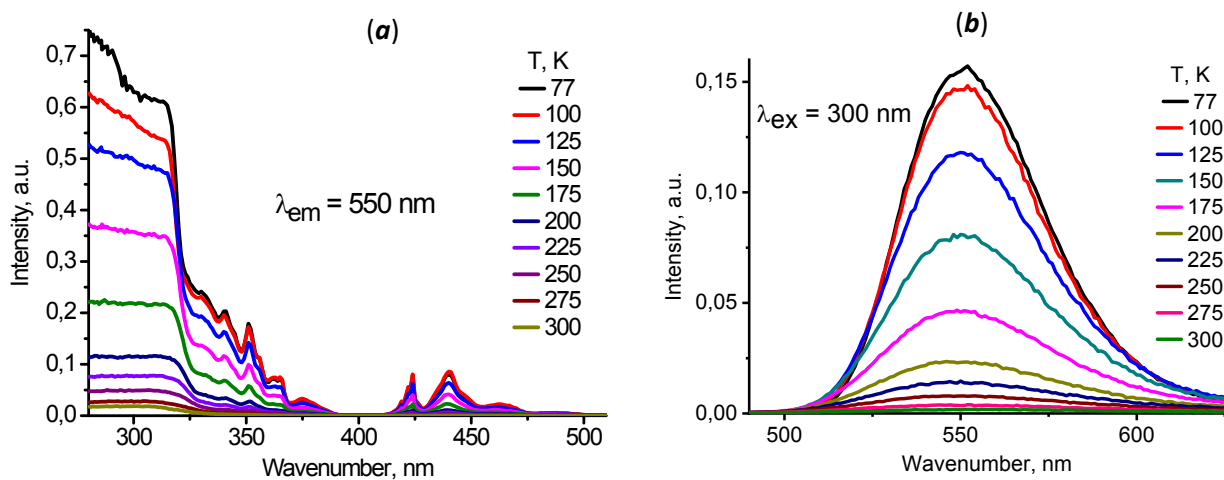


Figure S26. Temperature-dependant excitation (**a**) and emission (**b**) spectra for **1**.

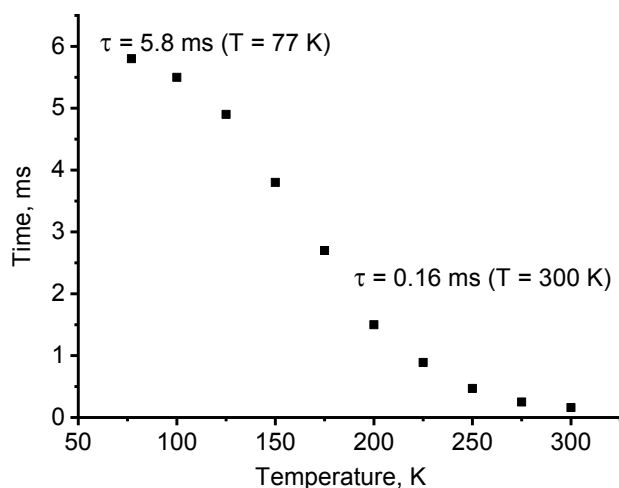


Figure S27. Emission lifetime against temperature plot for **1** ($\lambda_{\text{ex}} = 300 \text{ nm}$, $\lambda_{\text{em}} = 550 \text{ nm}$).

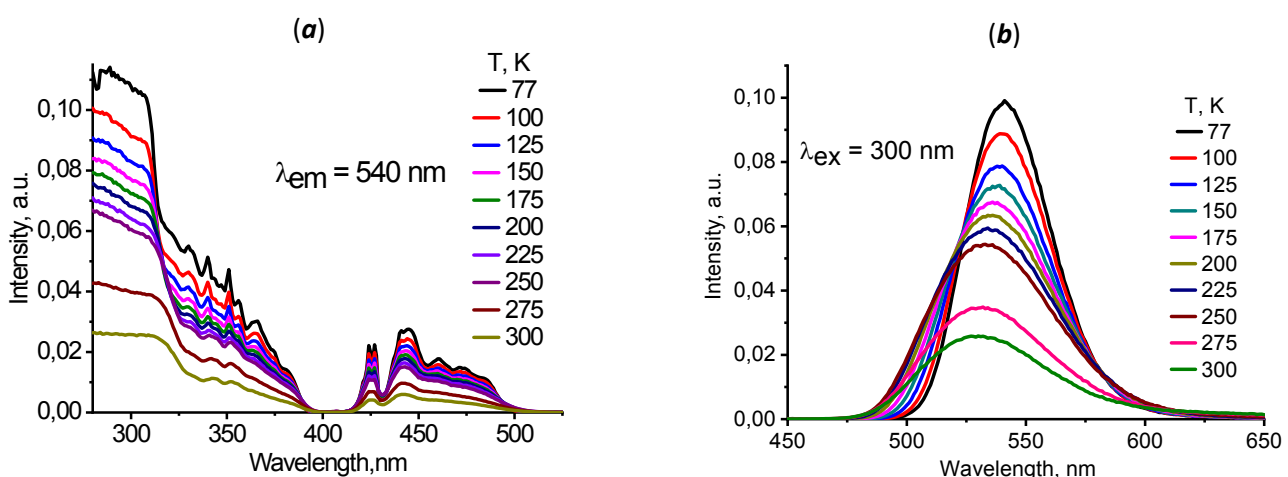


Figure S28. Temperature-dependant excitation (**a**) and emission (**b**) spectra for **2g**.

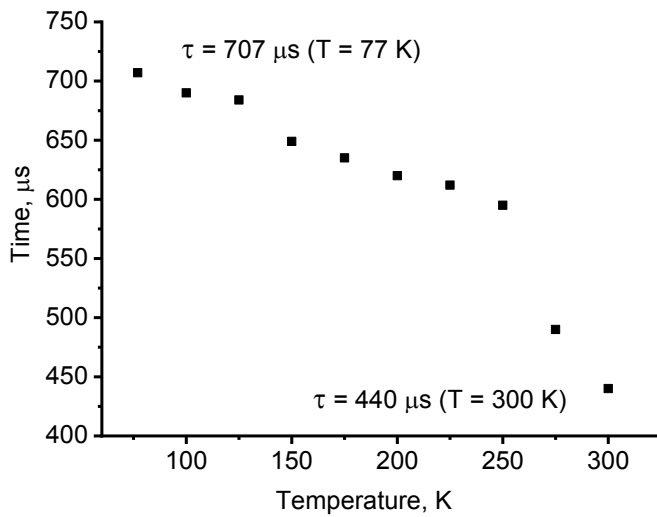


Figure S29. Emission lifetime against temperature plot for **2g** ($\lambda_{\text{ex}} = 300 \text{ nm}$, $\lambda_{\text{em}} = 540 \text{ nm}$).

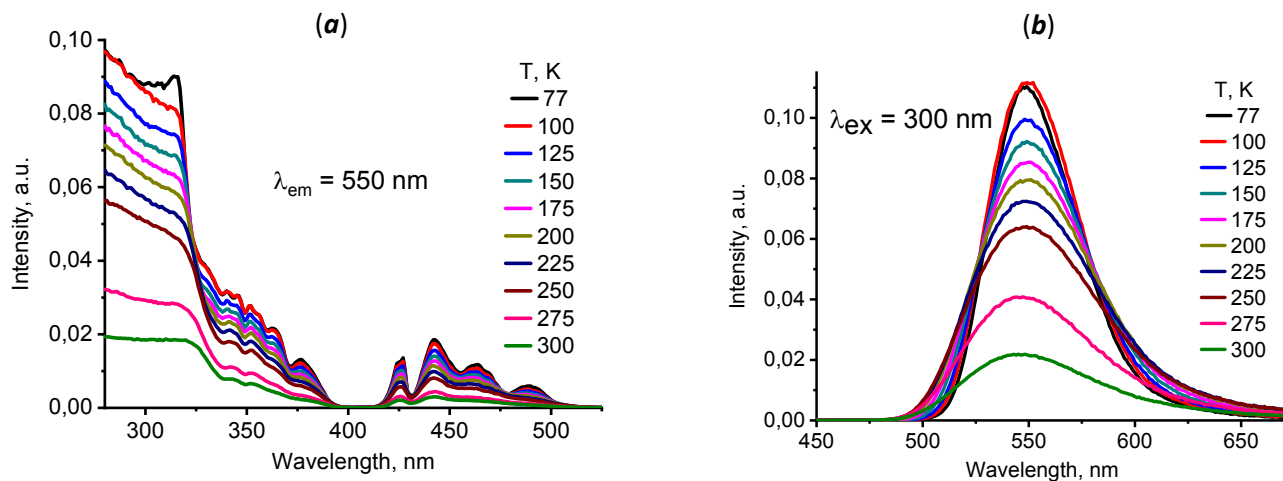


Figure S30. Temperature-dependant excitation (a) and emission (b) spectra for **2y**.

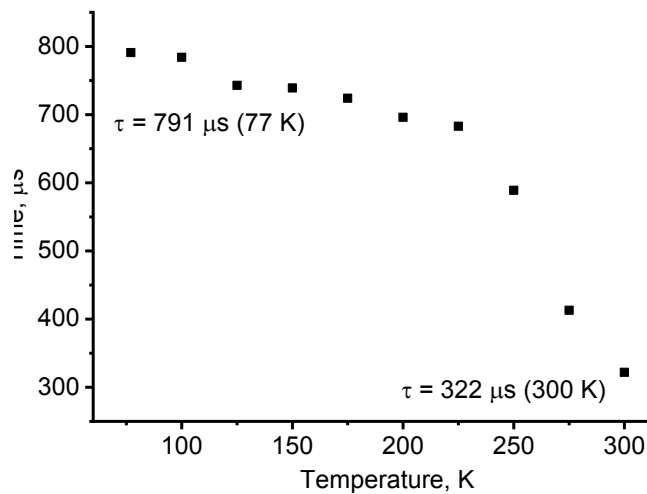


Figure S31. Emission lifetime against temperature plot for **2y** ($\lambda_{\text{ex}} = 300 \text{ nm}$, $\lambda_{\text{em}} = 550 \text{ nm}$).

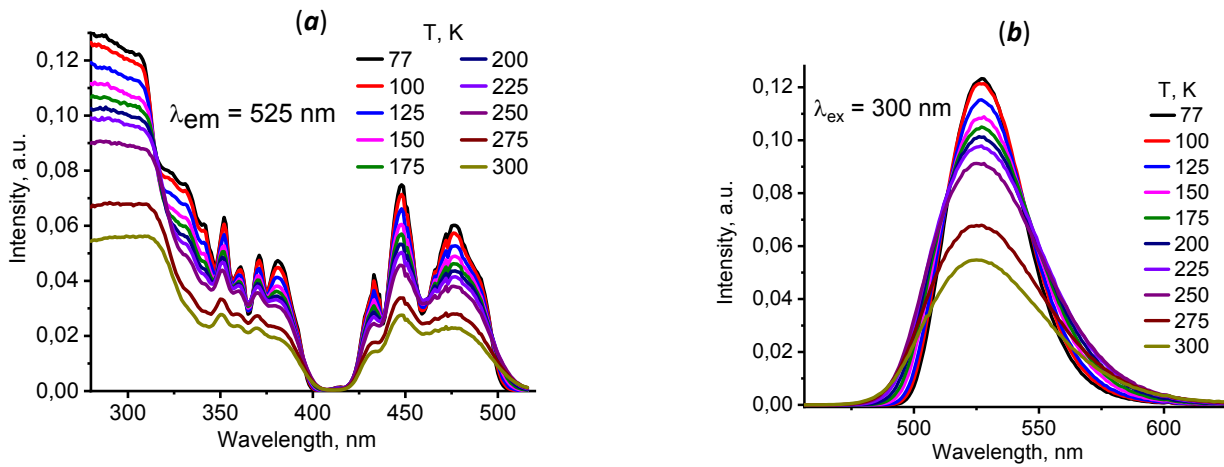


Figure S32. Temperature-dependant excitation (**a**) and emission (**b**) spectra for **3**.

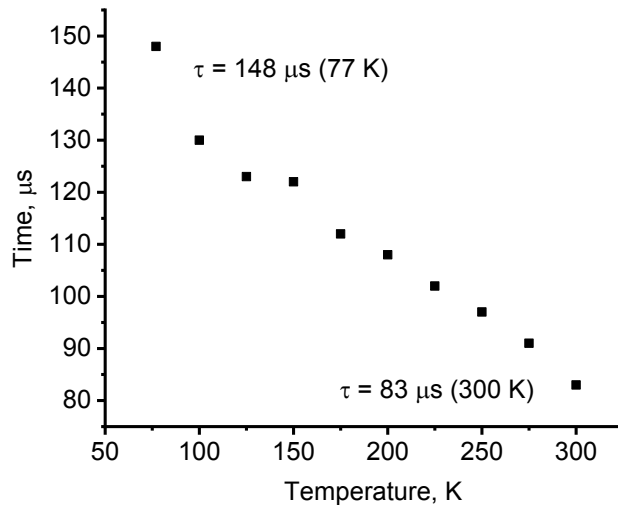


Figure S33. Emission lifetime against temperature plot for **3** ($\lambda_{\text{ex}} = 300 \text{ nm}$, $\lambda_{\text{em}} = 525 \text{ nm}$).

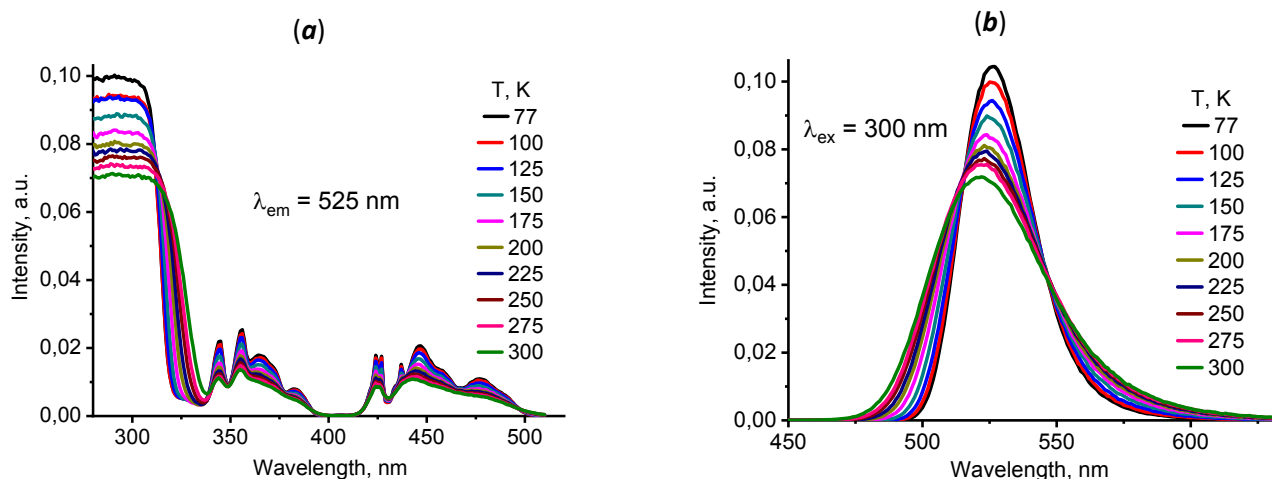


Figure S34. Temperature-dependant excitation (**a**) and emission (**b**) spectra for **4**.

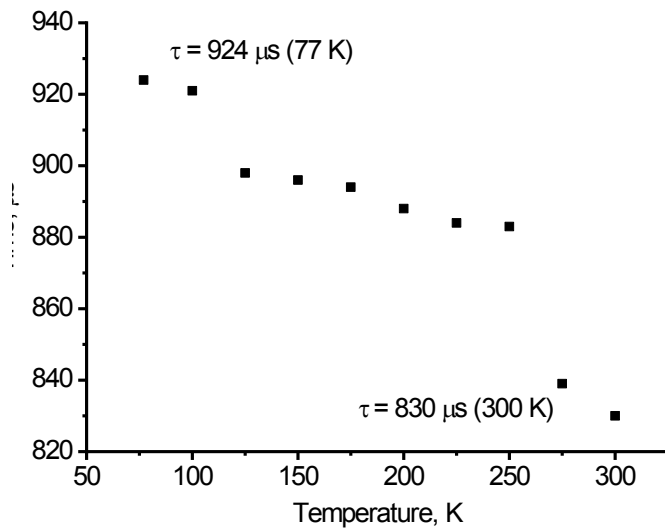


Figure S35. Emission lifetime against temperature plot for **4** ($\lambda_{\text{ex}} = 300 \text{ nm}$, $\lambda_{\text{em}} = 525 \text{ nm}$).

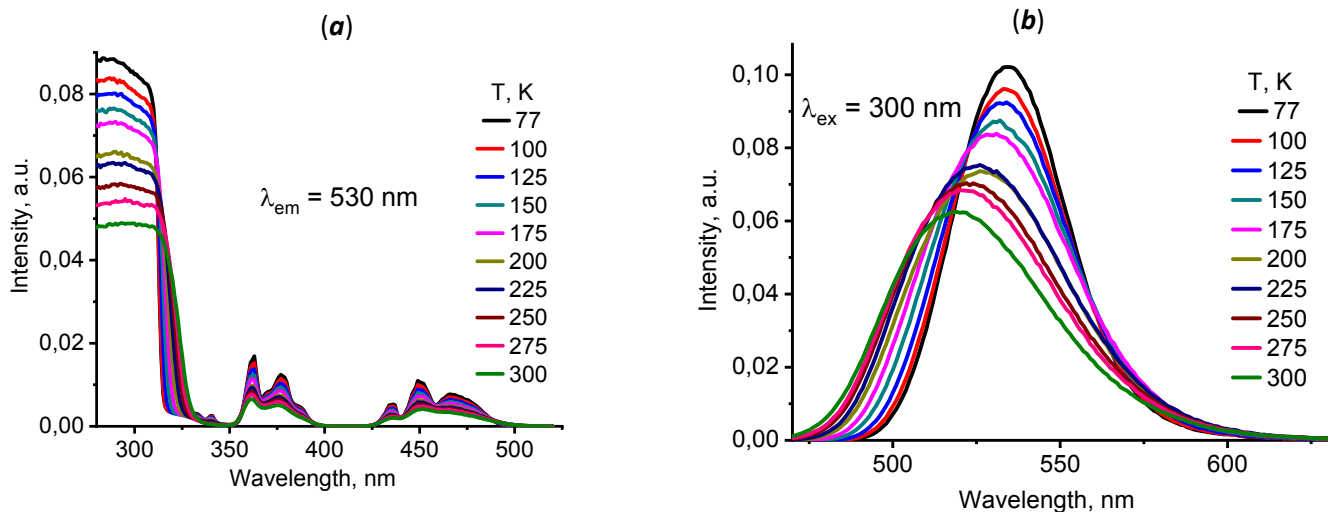


Figure S36. Temperature-dependant excitation (a) and emission (b) spectra for **5**· $\text{CH}_2\text{Cl}_2\cdot\text{H}_2\text{O}$.

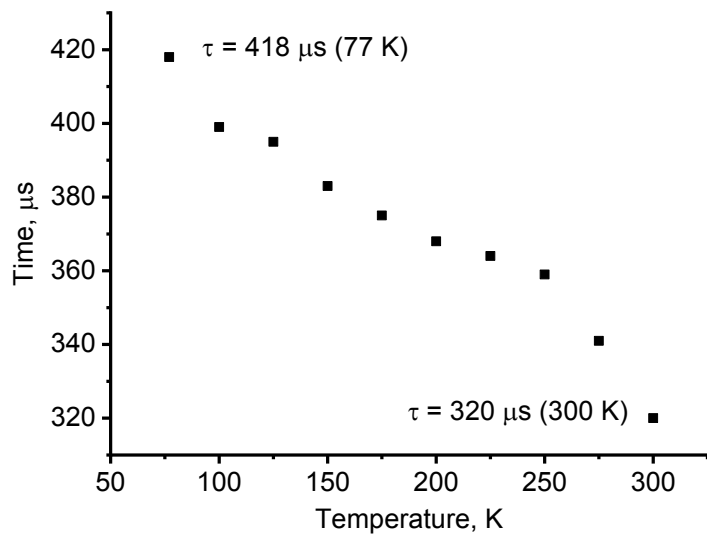


Figure S37. Emission lifetime against temperature plot for **5**· $\text{CH}_2\text{Cl}_2\cdot\text{H}_2\text{O}$ ($\lambda_{\text{ex}} = 300 \text{ nm}$, $\lambda_{\text{em}} = 530 \text{ nm}$).

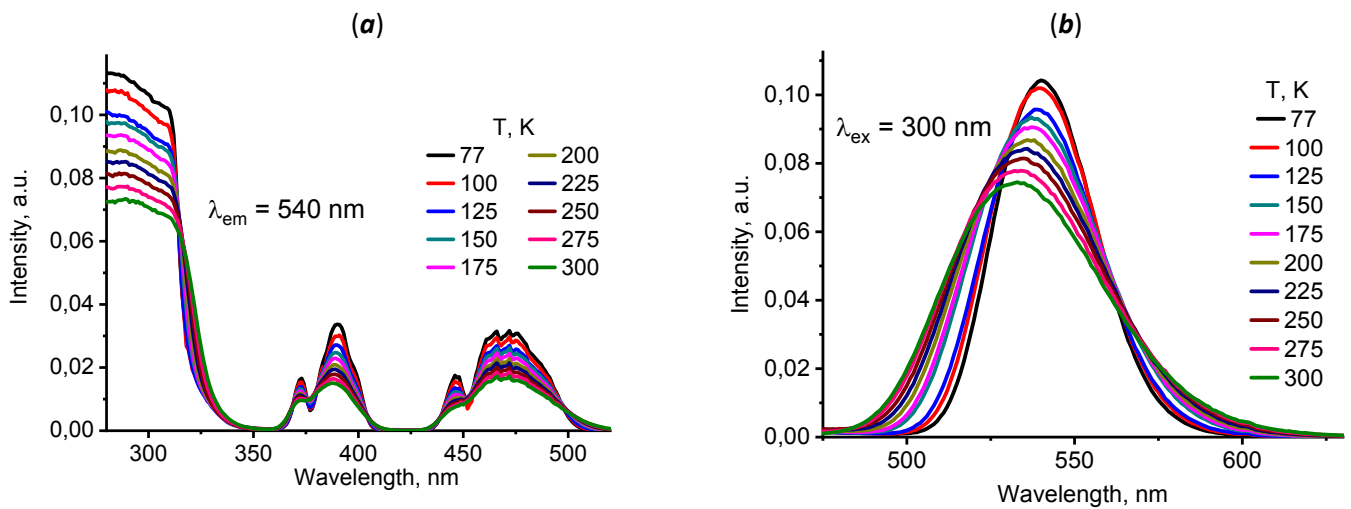


Figure S38. Temperature-dependant excitation (**a**) and emission (**b**) spectra for **6**.

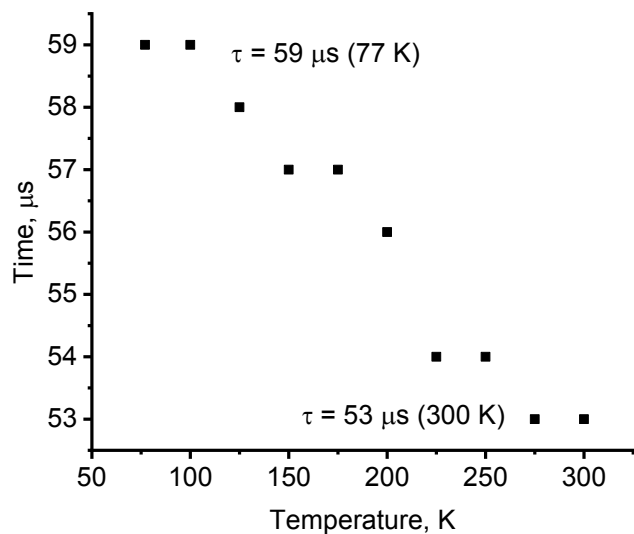


Figure S39. Emission lifetime against temperature plot for **6** ($\lambda_{\text{ex}} = 300 \text{ nm}$, $\lambda_{\text{em}} = 540 \text{ nm}$).

§8. Attempts to interconvert **2g** to

A series of experiments has been performed to carry out the solid-to-solid **2g** → **2y** and **2y** → **2g** transformations under the action of mechanical force, temperature, UV-light and VOCs. The following facts were established:

- a mechanical force (manual grinding of a powder with a pestle for 5 min) does not initiate a phase transition (PXRD and EA data). The same is true for the grinding of **2g** or **2y** in the presence of several drops of assistant solvent (MeOH, hexane, and CCl₄ were examined).
- The prolonged heating of **2g/2y** at 200 °C under vacuum (about 1 Torr) does not trigger its transition into **2y/2g**.
- The prolonged UV-irradiation (365 nm, 300 K) of solid **2g/2y** for overnight does not cause its transition into **2y/2g**.
- Similarly, the fuming of the solid samples **2g** and **2y** with VOCs does not initiate their interconversions. The solid sample of **2y/2g** (in a small open tube) was placed into a 30 mL vial, on the bottom of which about 1 mL of a volatile solvent was added. The vial was closed and exposed at ambient temperature for several days or a week. The anticipated **2g** → **2y** and **2y** → **2g** transitions were monitored by a UV flashlight and/or PXRD analysis. The following VOCs were tested: MeOH, *i*-PrOH, THF, DMF, acetone, MeCN, CHCl₃, and hexane. Moreover, water was used for this purpose. It turned out that compounds **2g** and **2y** tolerate vapors of *i*-PrOH, THF, and hexane. While the exposure of **2y/2g** under MeOH, DMF, or H₂O vapors results in the irreversible decomposition into unidentified products. Under acetone, MeCN, or CHCl₃ vapors, compounds **2g** and **2y** slowly turn into a non-emissive viscous solution.

§9. References

1. D. P. Pishchur and V. A. Drebushchak, *J. Therm. Anal. Calorim.*, **2016**, *124*, 951–958.
2. G. M. Sheldrick, *Acta Crystallogr., Sect. C: Struct. Chem.*, **2015**, *71*, 3–8.
3. *SADABS*, v. 2008-1, Bruker AXS, Madison, WI, USA, 2008.